Proceedings of the 25th International Conference on
Port and Ocean Engineering under Arctic Conditions
June 9-13, 2019, Delft, The Netherlands

Consideration of ice drift in determining the contribution of ice-induced vibrations to structural fatigue

Hayo Hendrikse[1], Jasper Koot[2],
[1] Delft University of Technology, Delft, The Netherlands
[2] Siemens Gamesa Renewable Energy, The Hague, The Netherlands

ABSTRACT

Ice-induced vibrations have to be considered in the design of vertically sided offshore structures which may encounter drifting sea or lake ice during their lifetime. One particular aspect is the contribution of ice-induced vibrations to the fatigue of such structures. Estimation of the duration of events is often difficult, due to limited available data on ice drift, leading to conservative assumptions.

In this paper, the approach followed for assessing the fatigue resulting from frequency lock-in vibrations in the design stage of a recent offshore wind project is presented. The project concerned offshore wind turbines with jacket support structures consisting partly of vertical structural members.

The severity of ice-induced vibrations for the structures is first assessed using a simulation model. Following this, ice drift is included in the assessment to obtain an estimate of the number of cycles of frequency lock-in over the lifetime of the structure. Results show that site-specific combinations of ice floe size and driving forces significantly influence the expected number of cycles of frequency lock-in. It is concluded that for this project limited conditions exist in which sustained vibrations can develop and that the contribution of frequency lock-in to structural fatigue is therefore limited as well.

KEY WORDS: Ice crushing, offshore wind, frequency lock-in, ice floe.

INTRODUCTION

For vertically-sided structures the dynamic ice-structure interaction is an important design consideration. Generally, intermittent crushing can govern ultimate limit state design and both intermittent crushing and frequency lock-in can have a significant contribution to fatigue. Full-scale experience with ice-induced vibrations has demonstrated the potential effects, but also the strong dependence on geographic location and structural properties (Blenkarn, 1970; Engelbrektson, 1987; Jefferies and Wright, 1988; Nordlund et al., 1988; Yue and Li, 2003). In the sub-Arctic regions, the location of many current offshore wind developments, the site-specific conditions determine to a large extent the contribution of ice-induced vibrations to structural fatigue.

For a recent offshore wind project in the Danish Nissum Bredning fjord (56^{o} 64' 69'', 8^{0} 27' 65.6", Figure 1) the development of ice-induced vibrations was investigated. The project consists of four 7 MW Siemens SWT-7.0-154 turbines with a rotor diameter of 154 m and hub height of 97.3 m. The support structures are jackets with three legs, of which two are executed with ice cones and one is close to vertical (Figure 2). During the project, the question arose as to the potential of frequency lock-in developing as a consequence of ice crushing on the one vertical leg, and the contribution of frequency lock-in to the fatigue of the structure.

In this paper, the results of the analysis of the structure with respect to frequency lock-in are presented. First, the severity of frequency lock-in is assessed using a simulation model for dynamic ice-structure interaction (Hendrikse and Nord, 2019). Results of this assessment are compared to observations on the JZ9-3 MDP in the Bohai Sea, and the ISO19906 (2018) approach. The influence of floe size, local current and wind, on the expected number of oscillation cycles is then studied, using a one-dimensional ice drift model.

Figure 1. Offshore wind turbines in ice at the Nissum Bredning site, winter 2018.

SIMULATION MODEL

For this project the simulation model presented in Hendrikse and Nord (2019) was used with project specific ice parameters. Input parameters for the ice and drift model are given in Table 1. The value for K_2 is chosen to obtain a peak global load in continuous brittle crushing equal to F_G, defined based on Eq.A.8-20 in ISO19906 (2018). With the vertical leg diameter of 1.77 m and a C_R value of 1.0 MPa this results in 5.5 10^5 N for 0.2 m ice thickness and 7.8 10^5 N for 0.3 m ice thickness.

Table 1. Ice and drift model input parameters used in combination with the model presented in Hendrikse and Nord (2019).

Ice model parameter	K_1/K_2	C_1/K_2	$C_2/K_2{}^3$	N	δ_f	r_{max}	K_2	
Value	0.26	0.94 s	3.2 10^{-5} m^2s	79	4 mm	6 mm	*	
Drift model parameter	ρ_w	$C_{d,w}$	ρ_a	$C_{d,a}$	v_w	v_a	d_i	h
Value	1025 kg m^{-3}	2.5 10^{-3}	1.29 kg m^{-3}	2 10^{-3}	0 up to 0.4 m s^{-1}	0 up to 18.3 m s^{-1}	500, 1000, 2000 m	0.2, 0.3 m

* Defined to obtain peak global ice load equal to F_G based on ISO19906 (2018).

The structure was modelled by considering the first ten vibrational modes as defined in Table 2. Modal amplitudes are mass-normalized. The ice was assumed to only act on the vertical leg shown in Figure 2 and any effects of the nearby cones, or ice action on the nearby cones is neglected in the simulations. The ice and structural model were solved in a coupled manner in the time domain as described in Hendrikse and Nord (2019). Ice was assumed to either approach the structure from the *x*- or *y*- direction with a 90-degree angle difference between them. The *x*-direction being along a line which crosses between the front two cones and hits the rear vertical member such that the third cone is exactly in the wake of the vertical member in Figure 2.

Table 2. Modal parameters used to describe the structure in the simulations.

Mode	Frequency (Hz)	Damping (% log decr.)	Modal amplitude x (-)	Modal amplitude y (-)
1	0.25	3.15	3.36 10^{-6}	3.45 10^{-7}
2	0.25	3.15	-3.68 10^{-6}	6.39 10^{-6}
3	1.01	6.0	-2.40 10^{-4}	8.33 10^{-5}
4	1.11	6.18	-5.40 10^{-4}	1.64 10^{-5}
5	1.12	6.43	1.02 10^{-5}	-5.70 10^{-4}
6	1.60	9.0	2.20 10^{-4}	-8.44 10^{-7}
7	1.94	11.9	-9.82 10^{-5}	-1.20 10^{-4}
8	2.04	11.2	6.90 10^{-4}	-4.30 10^{-4}
9	4.26	20	2.60 10^{-4}	-8.97 10^{-7}
10	4.61	20	-8.02 10^{-6}	3.00 10^{-4}

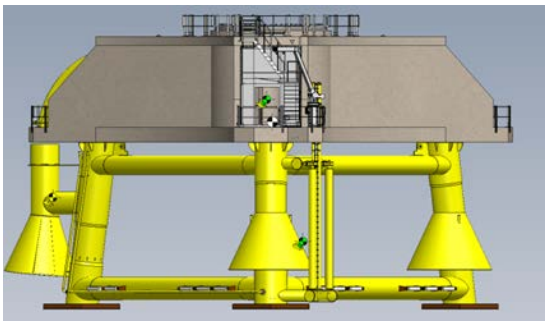

Figure 2. Foundation concept with a single leg on the left for which ice crushing has to be considered.

ASSESSMENT OF SEVERITY OF FREQUENCY LOCK-IN

The general susceptibility of the structure to frequency lock-in was assessed by running the simulation model with assumed constant ice drift speeds in the range of 0.01 up to 0.15 m s^{-1}. Figure 3 shows the peak structural velocity plotted against ice drift speed for the two ice thicknesses considered and the ice load applied in x- and y-direction respectively. As defined in the work by Toyama et al. (1983), during frequency lock-in the peak structural velocity is generally a factor 1.0 up to 1.5 times the ice drift speed (area between straight lines). Differences for the load applied in x- or y-direction are small as modal properties do not differ significantly for the two directions. Maximum drift speeds where frequency lock-in develops are 0.045 m s^{-1} for 0.02 m thick ice, and 0.05 m s^{-1} for 0.03 m thick ice.

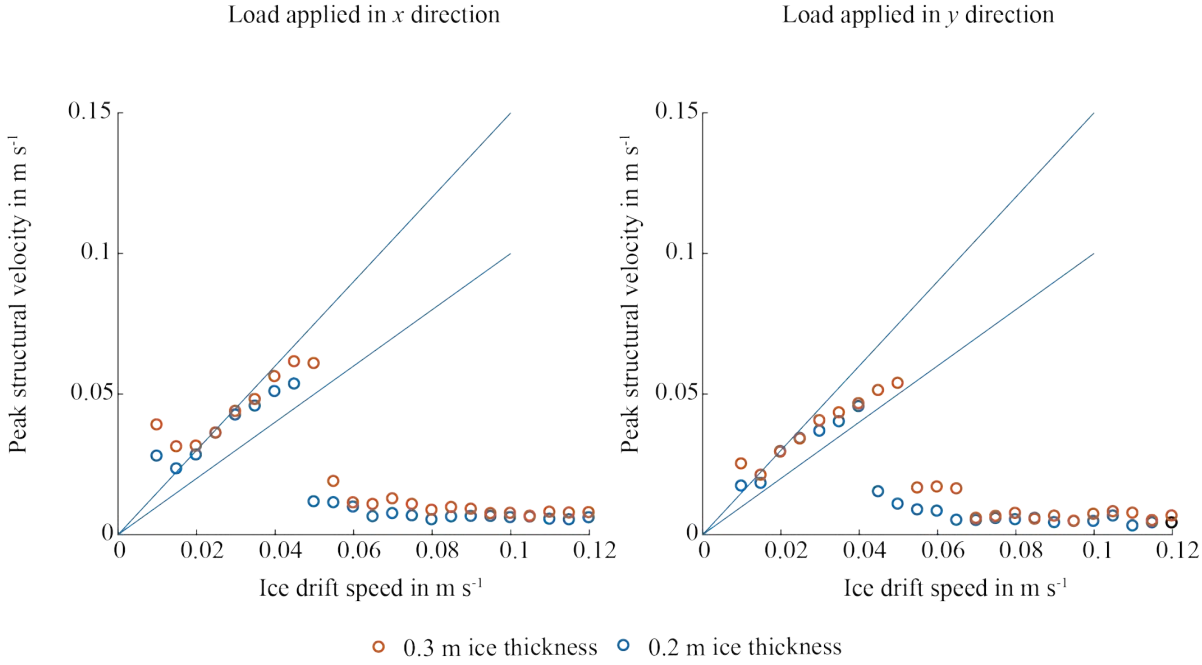

Figure 3. Peak structural velocity at the ice action point versus ice drift speed for two ice thicknesses considered. Ice load applied in x-direction (left) and ice load applied in y-direction are shown (right). The straight lines bound the range of amplitudes typically associated with frequency lock-in.

Time traces of structural displacement at the ice action point, structural velocity at the ice action point, and global ice load for the most severe case of frequency lock-in (x-direction, 0.3 m ice thickness, 0.05 m s^{-1} drift speed) are shown in Figure 4. An effect was found which is not always observed during frequency lock-in and originates from the specific structural properties of the Nissum Bredning support structure. There is a clear interference which stems from multiple structural modes simultaneously interacting with the ice. Scrutiny of the structural response reveals that lock-in develops in the second bending mode at 1.1 Hz. However, a beating effect with a 0.1 Hz beat frequency is also visible indicating that the torsional mode at 1.0 Hz is also active. A consequence of this is a deviation from the quasi-sinusoidal displacement pattern of the structure, but more importantly an increase in amplitude of oscillation of the structure compared to lock-in where only a single mode is active, visible along the negative axis in the structural velocity plot.

The results obtained for the Nissum Bredning structure are compared to full-scale observations of the JZ9-3 MDP mooring pile in the Bohai Sea (Yue et al., 2009). This mooring pile has a waterline diameter of 1.5 m (larger including the installed load panels) and regularly encounters ice with a thickness up to 0.3 m. The first natural frequency of the pile is 2.31 Hz. The waterline

stiffness of the structure is reported as 4.86 10^7 N m^{-1}. Damping values have not been reported in literature; however, decaying oscillation patterns indicate a value below 1.5 percent of critical which is comparable to the damping in the second bending mode of the Nissum Bredning structure.

Reports of ice-induced vibrations of JZ9-3 MDP indicate frequency lock-in to have occurred for the pile for drift speeds in the range of 0.01 up to 0.04 m s^{-1}. Considering that the second mode of the Nissum Bredning structure has a lower natural frequency than and equal damping as the JZ9-3 MDP, it is to be expected that lock-in can develop up to higher ice drift speeds in similar ice conditions (Hendrikse, 2017). An opposite trend would be expected from the significantly larger oscillating mass (or lower modal amplitude) for the Nissum Bredning structure (3.4 10^6 kg) compared to the JZ9-3 MDP (1.25 10^5 kg). The simulations for the Nissum Bredning structure showing a somewhat higher drift speed for frequency lock-in than observed in full-scale for the JZ9-3 MDP is considered reasonable, given that the expected effects of differences in structural properties having an opposite impact on the maximum drift speed for frequency lock-in.

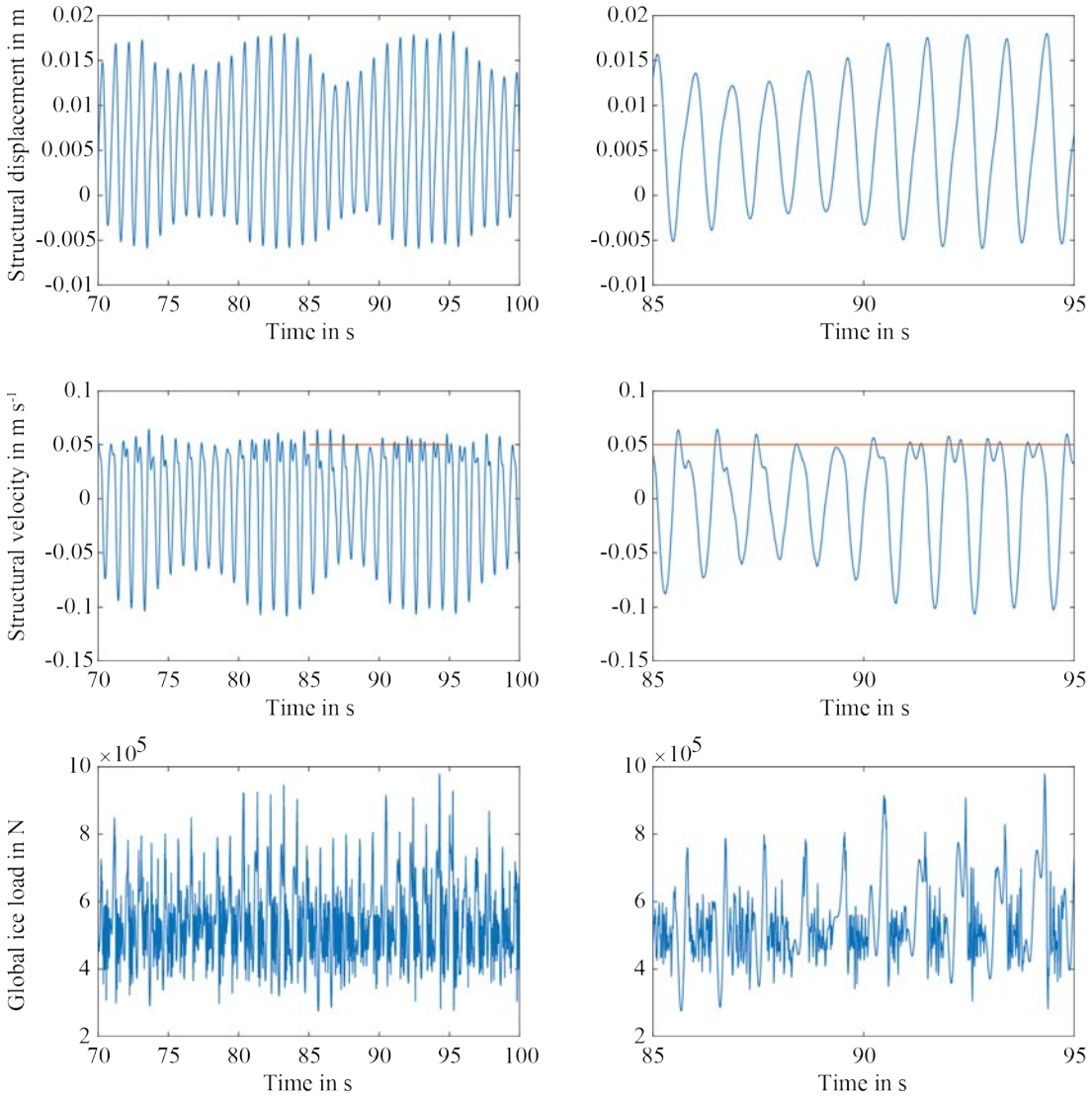

Figure 4. Structural displacement, velocity, and global ice load during frequency lock-in for 0.3 m ice thickness at 0.05 m s^{-1} with the load applied in *x*-direction. The longer duration signal shows an interference effect. The red line indicates the constant ice drift speed.

A comparison was also made between the structural response and ice load during frequency lock-in obtained from the model simulations, and simulations using the simplified forcing function defined in ISO19906 A.8.2.6.1 (2018). The scenario is a 0.3 m thick ice sheet at constant drift speed of 0.05 m s^{-1}. The ISO19906 method defines that the structural amplitude at waterline should be 0.07 m s^{-1} in this scenario, including a safety factor for design. The requirement needs to be met by adjusting the factor q in the ice load description:

$$F(t) = (1 - q)F_g + \frac{qF_g(x_s(t)-1)}{2} \quad \text{(Eq. 1)}$$

Where:

$$x_s(t) = t \pmod 1 \quad \text{(Eq. 2)}$$

is the sawtooth wave. For this particular case a factor q of 0.14 is found which falls in the range specified in ISO19906 (0.1 – 0.5) in which case frequency lock-in can develop.

A comparison of time traces between the model and ISO19906 approach is shown in Figure 5 where the amplitude of oscillation at the waterline is slightly higher for the displacement obtained from the simulations, resulting from the larger negative structural velocities which develop. The most obvious difference is observed in the load patterns where the ISO19906 load has a higher mean value compared to the simulated load. This is important as it may affect the fatigue contribution for concrete structures, for which the mean stress is to be included in the calculations. The peak loads in the simulated load signal exceed the ISO19906 maximum load by about 25% which is considered realistic for compliant structures experiencing frequency lock-in (Gravesen and Kärnä, 2009).

From this analysis it is concluded that frequency lock-in can develop for the Nissum Bredning structures for ice thicknesses of 0.2 and 0.3 m, at ice drift speeds between 0.015 m s^{-1} and 0.045 m s^{-1} and 0.015 m s^{-1} and 0.05 m s^{-1}, respectively.

CONTRIBUTION OF FREQUENCY LOCK-IN TO STRUCTURAL FATIGUE

To determine the contribution of frequency lock-in to structural fatigue the common approach is to first assign probabilities to relevant combinations of ice thickness and ice drift speed. Based on the assessment presented in the previous section it can be determined which of these combinations include ice drift speeds leading to frequency lock-in. With the assumption of a constant ice drift speed frequency lock-in is then assumed, in case the ISO19906 approach is used, or found to last, in case simulations are performed, for the entire duration of a simulation. In a typical 10-minute simulation this adds up to about 660 cycles per simulation for the Nissum Bredning structure, estimated based on Figure 5. The amplitude of oscillation can then be estimated as 1.4 times the ice drift speed divided by the natural frequency of the mode at which frequency lock-in develops ω_n, after which an estimate for the fatigue contribution can be easily made.

The assumption of a constant ice drift speed can have a significant impact on the number of vibration cycles. In reality, only unique combinations of driving forces, floe sizes, and ice concentrations would result in stable drift speeds of an ice floe in interaction with a structure over a 10-minute duration interval. The driving forces and expected ice floe sizes at the Nissum Bredning site were investigated with the aim of identifying the conditions leading to stable drift speeds in the range of critical speeds for frequency lock-in as found in the previous section. For this analysis the drift model based on the work by Leppäranta (2011) was used as defined in Hendrikse and Nord (2019).

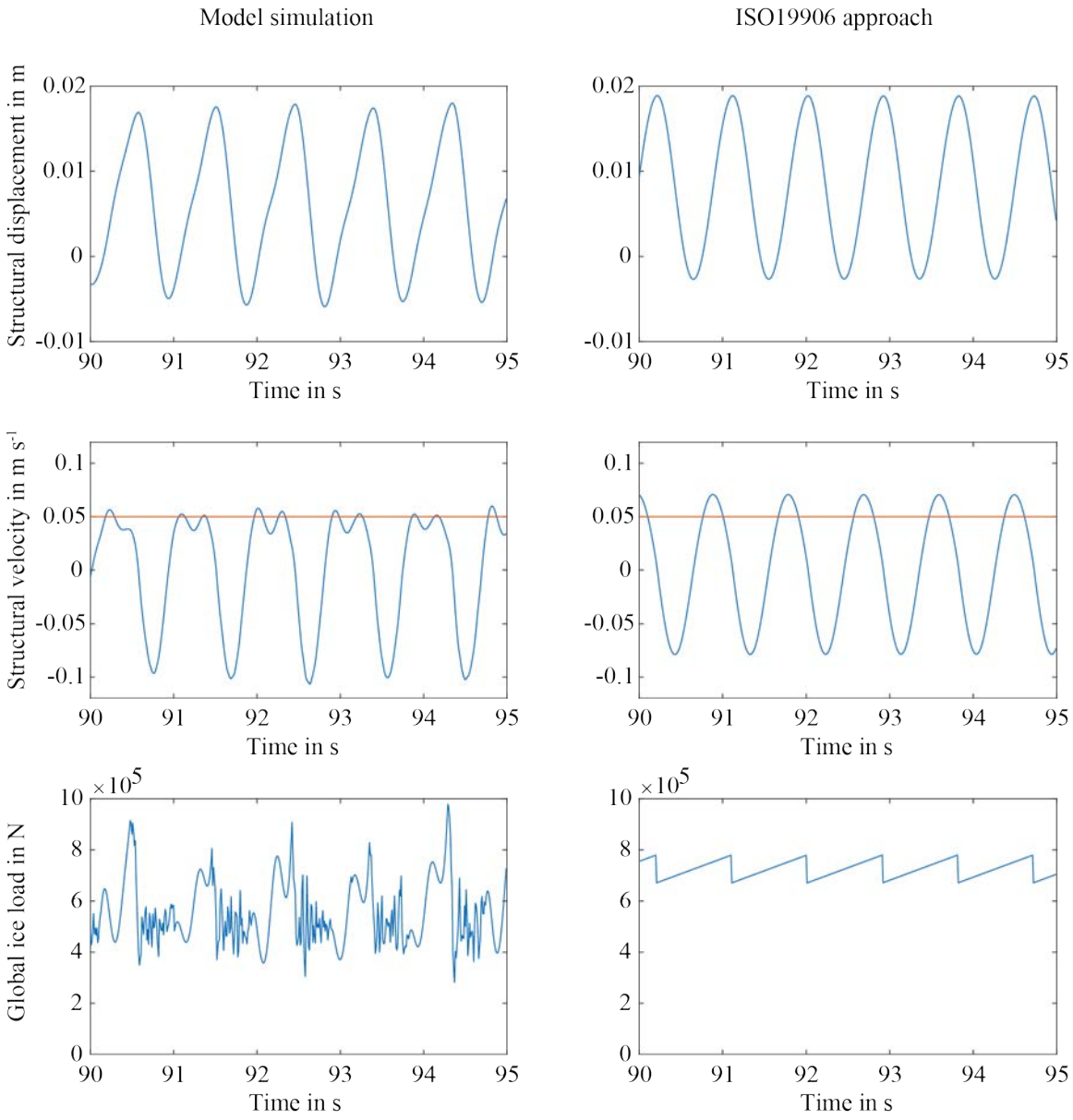

Figure 4. Comparison of frequency lock-in for 0.3 m thick ice at 0.05 m s^{-1} constant drift speed simulated with the model (left) and based on the ISO19906 approach (right). Structural displacement, velocity, and global ice load are shown. The red line indicates the magnitude of the constant ice drift speed.

The equilibrium ice drift speed of an ice floe under the influence of driving forces and the resistance from the Nissum Bredning structure as the floe crushes against it was first obtained (Hendrikse and Nord, 2019). Contour plots for the relevant combinations of ice thickness (0.2 and 0.3 m) and floe size (1000, 1500, and 2000 m) are presented in Figure 6, where the green areas indicate an equilibrium drift speed in the critical range for sustained frequency lock-in (0 m s^{-1} up to 0.05 m s^{-1}). The vertical axis in Figure 6 covers the range of current speeds possible at the site, and the horizontal axis the range of possible wind speeds at 10 m above sea level. The analysis showed that all floes smaller than 590 m equivalent diameter will come to a stop during interaction. These floes will therefore only result in a small number of cycles of frequency lock-in during the time where they slow down as a result of the interaction with the structure. For the larger ice floes in the range above 1500 m equivalent diameter, there is a chance of sustained frequency lock-in when the current speed exceeds 0.2 m s^{-1} and there is limited to no wind (< 8 m s^{-1}).

Based on the assessment it is concluded that conditions of sustained vibrations may develop, but that for the majority of combinations of floe size, wind speed and current speed it is expected that the ice sheet comes to a stop during interaction or remains at a high drift speed leading to continuous brittle crushing.

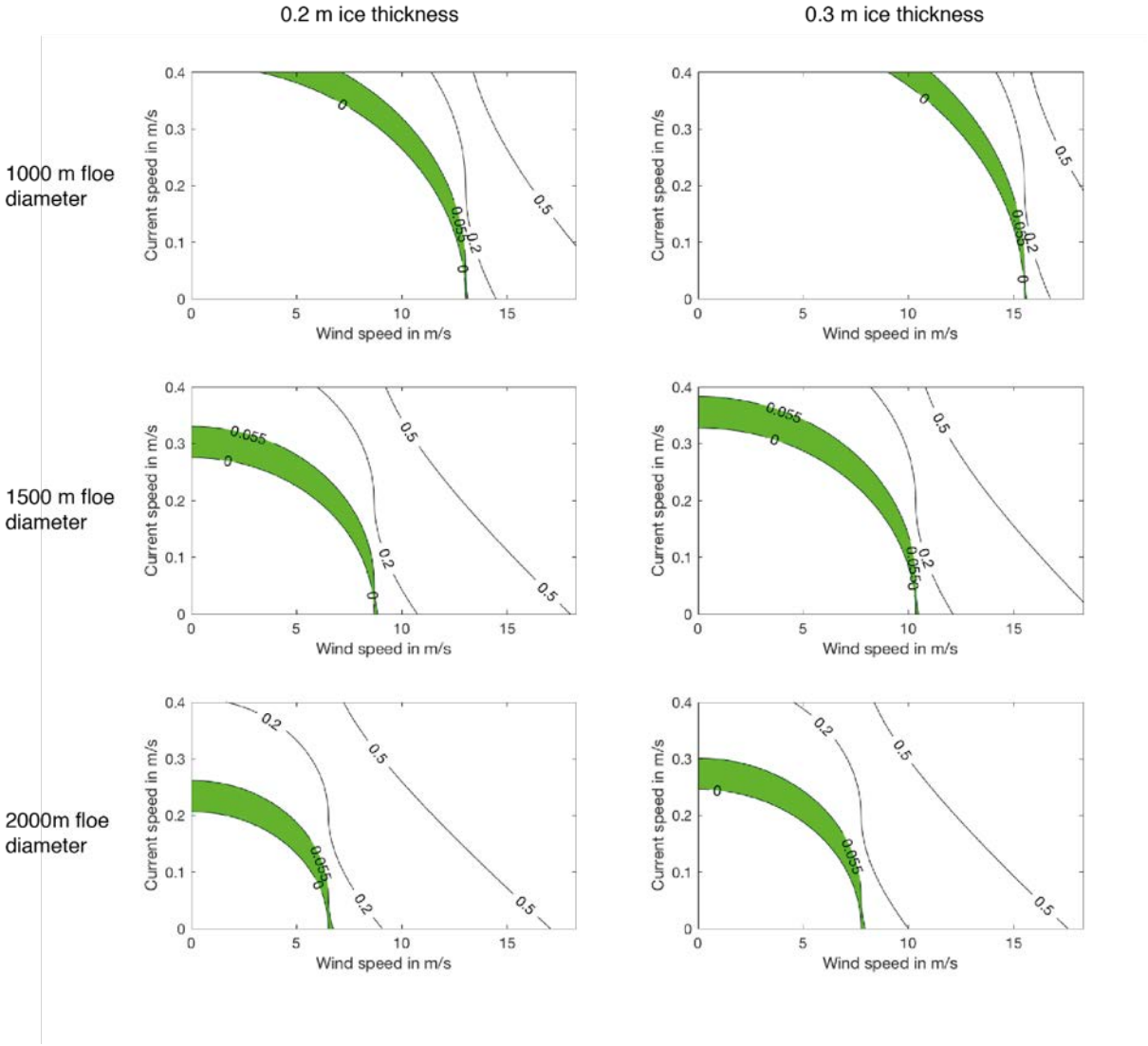

Figure 5. Contour plot of the equilibrium drift speed as a function of wind and current speed for 0.2 and 0.3 m ice thickness, and 1000, 1500, and 2000 m diameter ice floes. The green regions indicate parameter combinations for which sustained frequency lock-in may develop for the Nissum Bredning structure based on the analysis in the previous section. Note: the ranges are approximate as during frequency lock-in and intermittent crushing the ice load is generally larger in magnitude than assumed for this analysis, shifting the green areas to higher wind speeds and higher current speeds.

An indication of the expected number of cycles of frequency lock-in was obtained for a typical current speed at the Nissum Bredning location of 0.2 m s^{-1} and wind speeds in the range of 0 to 15 m s^{-1} (Steps of 1 m s^{-1}) for a 2 km equivalent diameter ice sheet of 0.3 m thickness. For each simulation the number of cycles in frequency lock-in was determined from the local maxima of the displacement time trace based on the requirement that consecutive peaks should lie within 80 to 120 percent of the natural period for which frequency lock-in develops and the

peak-to-peak amplitude should at least equal that expected for the lowest ice drift speed at which frequency lock-in can develop:

$$\hat{x} > 2\frac{v_{fli;min}}{\omega_{fli}} \quad \text{(Eq. 3)}$$

For the initial condition the ice sheet was taken either at rest against the structure, or in equilibrium with the environmental driving forces. Note that this analysis does not replace a full fatigue analysis as only the displacement cycles were counted.

Results for the ice sheet initially at rest show the dependence of the number of cycles of frequency lock-in on wind speed (Table 3). Up to 7 m s^{-1} wind speed the ice sheet stays at rest and deforms in a creep like manner, resulting in one or two cycles of low amplitude frequency lock-in. The most severe case develops at 7 m s^{-1} wind speed resulting in 503 cycles (almost the full duration of the 10-minute simulation) with the majority at high amplitudes. For wind speeds above 7 m s^{-1} the number of cycles reduces as the ice sheet accelerates faster and spends less time in the range of speeds which can cause frequency lock-in. For 15 m s^{-1} wind, no more cycles are observed.

A comparison can be made with the results for an ice sheet drifting towards the structure initially being in equilibrium with the environmental driving forces (Table 4). For wind speeds below 3 m s^{-1} the ice floe slows down and comes to a stop in the 10-minute interval, resulting in a small number of cycles of low amplitude frequency lock-in. For wind speeds between 3 m s^{-1} and 7 m s^{-1} the ice sheet does not reach a low enough drift speed for frequency lock-in to be observed during the 10-minute simulation. For wind speeds above 7 m s^{-1} the ice drift speed remains above the critical drift speed for frequency lock-in. Note that the single cycle occurs as a result of the initial impact between the ice floe and the structure.

Comparing the results in Tables 3 and 4 shows that the most severe 10-minute cases are those where an ice sheet at rest is accelerated by the environmental driving forces. The number of cycles in a 10-minute simulation shows a strong dependence on wind and current speed, with only specific combinations resulting in a large number of high amplitude cycles.

It is noted that the choice for 10-minute simulations, typical for simulations with wind signals on the wind turbines, might underestimate the number of cycles in Table 4 as the floes do not slow down enough for frequency lock-in to start yet. Longer simulations, or different initial conditions will show more cycles of vibrations, showing the strong dependence of the number of cycles on local ice and drift conditions.

Table 3. Cycles of frequency lock-in for 0.2 m s^{-1} current speed and different constant wind speeds. 0.3 m ice thickness, 2000 m floe diameter, initially at rest.

0.3 m, 2000 m, at rest accelerating ice floe	Wind speed (m s^{-1})															
Amplitude range of structural displacement at the ice action point (mm)	0	1	2	3	4	5	6	7	8	9	10	11	12	13	14	15
6 - 8	0	0	0	0	0	1	1	3	14	12	12	10	11	13	12	0
8 - 11	0	0	0	0	0	1	0	41	27	20	13	13	12	8	11	0
11 - 13	0	0	0	0	1	0	0	70	31	21	14	14	11	10	7	0
13 - 16	0	0	0	0	0	0	0	87	34	25	17	13	11	12	10	0
16 - 18	0	0	0	0	0	0	0	97	89	44	39	23	16	24	10	0
18 - 21	0	0	0	0	0	0	0	116	95	55	34	20	22	14	7	0
21 - 23	0	0	0	0	0	0	0	84	48	30	19	11	16	12	7	0
23 - 26	0	0	0	0	0	0	0	5	15	4	1	8	2	7	2	0
26 - 28[1]	0	0	0	0	0	0	0	0	0	4	0	0	3	0	0	0
28 - 31	0	0	0	0	0	0	0	0	0	0	0	0	0	0	0	0
Sum	0	0	0	0	1	2	1	503	353	215	149	112	104	100	66	0

[1] Maximum amplitude range for the Nissum Bredning structure based on the ISO19906 (2018) approach.

Table 4. Cycles of frequency lock-in for 0.2 m s^{-1} current speed and different constant wind speeds. 0.3 m ice thickness, 2000 m floe diameter, initially at equilibrium with the driving forces.

0.3 m, 2000 m, in equilibrium Decelerating ice floe	Wind speed (m s^{-1})															
Amplitude range of structural displacement at the ice action point (mm)	0	1	2	3	4	5	6	7	8	9	10	11	12	13	14	15
6 - 8	5	9	3	1	1	1	1	1	1	1	1	1	1	1	1	1
8 - 11	14	18	17	0	0	0	0	0	0	0	0	0	0	0	0	0
11 - 13	17	19	23	0	0	0	0	0	0	0	0	0	0	0	0	0
13 - 16	15	17	19	0	0	0	0	0	0	0	0	0	0	0	0	0
16 - 18	17	14	14	0	0	0	0	0	0	0	0	0	0	0	0	0
18 - 21	2	0	1	0	0	0	0	0	0	0	0	0	0	0	0	0
21 - 23	0	0	0	0	0	0	0	0	0	0	0	0	0	0	0	0
23 - 26	0	0	0	0	0	0	0	0	0	0	0	0	0	0	0	0
26 - 28[1]	0	0	0	0	0	0	0	0	0	0	0	0	0	0	0	0
28 - 31	0	0	0	0	0	0	0	0	0	0	0	0	0	0	0	0
Sum	70	77	77	1	1	1	1	1	1	1	1	1	1	1	1	1

[1] Maximum amplitude range for the Nissum Bredning structure based on the ISO19906 (2018) approach.

DISCUSSION

Results of the frequency lock-in analysis for the Nissum Bredning structure and site show that the conditions for sustained frequency lock-in are very limited and for the relevant ice conditions the majority of interaction events is likely to lead only to a limited number of cycles of oscillation of the structure. Frequency lock-in is therefore not expected to cause significant fatigue damage. In order to determine the exact contribution to fatigue it is required to define relevant combinations of equivalent ice floe size, wind speed, and current speed and assign corresponding probabilities of occurrence. For each of the relevant combinations, simulations are then to be made to determine the contribution to fatigue of the structure. This analysis is not presented here.

Sustained frequency lock-in vibrations have been observed in the Bohai Bay (Yue et al. 2001) and for example for the oil and gas platforms offshore Sakhalin. From Figure 6 it can be seen that for larger equivalent floe size the required driving forces for sustained frequency lock-in are smaller as the green area moves to the origin of the plot. At such offshore locations where the pack ice is large in extent and it is driven by tidal currents the analysis presented here suggests that periods of sustained vibrations indeed may develop much more often. The Norströmsgrund lighthouse in the Gulf of Bothnia only showed limited duration events in interaction with ice (Nord et al. 2018). As the ice drift is more wind driven for this location the conditions for sustained vibrations are indeed expected to be limited based on Figure 6, and most observed events are likely to have been accelerating or decelerating ice sheets resulting in a small number of cycles of frequency lock-in (Table 3 and Table 4).

The analysis presented does not consider water level changes, resulting in different application points of the load to the structure which may result in more severe vibrations. Limiting effects of nearby cones and turbine operation were also not considered in the analysis. In all simulations, it was assumed that intact ice acts over the entire width of the vertical leg of the jacket. Limiting mechanisms such as ice buckling, bending and splitting, which may develop for smaller floes (Hendrikse and Metrikine, 2016; Lu et al., 2016) were not considered. It is further noted that intermittent crushing and continuous brittle crushing also contribute to the total fatigue of the structure. These can be included in a similar manner as presented here for frequency lock-in.

CONCLUSION

Analysis of the Nissum Bredning structure shows that the structure is susceptible to frequency lock-in at constant ice drift speeds between 0.015 and 0.05 m s^{-1} for ice with a thickness up to 0.3 m. Due to the unique structural properties of the Nissum Bredning structure, the interaction between the ice and multiple structural modes may result in displacement and velocity amplitudes during frequency lock-in that exceed values commonly assumed in approaches considering interaction with only a single mode. The response of the structure in this case deviates significantly from a harmonic oscillation.

The drift analysis shows that, for all floes smaller than 590 m equivalent diameter, there is no chance of sustained frequency lock-in. For floes in the range of 1000 up to 2000 m equivalent diameter, there is a chance of sustained frequency lock-in in conditions where the current speed exceeds 0.2 m s^{-1} and the wind speed is below 8 m s^{-1} approximately. It is found that the predicted number of cycles of frequency lock-in depends on the initial conditions assumed for the ice floe either being at rest against the structure, drifting in equilibrium with the environmental driving forces, or anything in between.

Results of the analysis show that in general the contribution of frequency lock-in to structural fatigue depends significantly on site-specific environmental conditions. At locations where the ice extent is significant and its drift is mainly governed by currents it is likely that structures experience long periods of sustained vibration, provided these structures are susceptible to ice-induced vibrations. At locations where the ice floe size is typically small and wind is the main driving force sustained vibrations are not likely to develop and typical interaction events consist only of a limited number of vibration cycles as ice sheets accelerate or decelerate during interaction.

ACKNOWLEDGEMENTS

The authors thank the Nissum Bredning demonstrator project and Siemens Gamesa Renewable Energy for the use of project information in this article.

The authors thank mr. Cody C. Owen for his contribution in running simulations for this project.

REFERENCES

Blenkarn, K.A., 1970. Measurements and analysis of ice forces on Cook Inlet structures. Proceedings of the Second Annual Offshore Technology Conference, volume II, 365-378, Houston, Texas.

Engelbrektson, A., 1987. Analysis of field observations from Norströmsgrund lighthouse during the period 1979-1985. A. Study project ice forces against offshore structures. VBB Project M7334. Report, No 2. Jan 15.

Gravesen, H., Kärnä, T., 2009. Ice loads for offshore wind turbines in southern Baltic Sea. Proceedings of the 20th International Conference on Port and Ocean Engineering under Arctic conditions, POAC09-3, 12p.

Hendrikse, H., 2017. Ice-induced vibrations of vertically sided offshore structures. PhD thesis. Delft University of Technology.

Hendrikse, H., Metrikine, A., 2016. Ice-induced vibrations and ice buckling. Cold. Reg. Sci. Technol. 131, pp. 129-141.

Hendrikse, H., Nord, T., 2019. Dynamic response of an offshore structure interacting with an ice floe failing in crushing. Mar. Struct. 65, pp. 271-290.

ISO19906, 2018. Petroleum and Natural Gas Industries - Arctic Offshore Structures. FDIS-2018(E), 30-04-2018.

Jefferies, M.G., Wright, W.H., 1988. Dynamic response of 'Molikpaq' to ice-structure interaction. Proceedings of the Seventh Internatinoal Conference on Offshore Mechanics and Arctic Engineering, volume 4, 201-220, Houston, Texas.

Leppäranta, M., 2011. The Drift of Sea Ice (Second Edition). SPRINGER-PRAXIS BOOKS IN GEOPHYSICAL SCIENCES, ISBN 978-3-642-04682-7, 370 p.

Lu, W., Lubbad, R., Løset, S., Kashafutdinov, M., 2016. Fracture of an ice floe: Local out-of-plane flexural failure versus global in-plane splitting failure. Cold. Reg. Sci. Technol. 123, pp. 1-13.

Nord, T.S., Samardzija, I., Hendrikse, H., Bjerkås, M., Høyland, K.V., Li, H., 2018. Ice-induced vibrations of the Norströmsgrund lighthouse. Cold reg. sci. technol., 155:237-251.

Nordlund, O.-P, Kärnä, T., Järvinen, E., 1988. Measurements of ice-induced vibrations of channel markers. Proceedings of the Ninth IAHR International Sympoisum on Ice, volume 1, 537-548, Sapporo, Japan.

Toyama, Y., Sensu, T., Minami, M., Yashima, N., 1983. Model tests on ice-induced self-excited vibration of cylindrical structures. Proceedings of the Seventh International Conference on Port and Ocean Engineering under Arctic Conditions, volume 2, 834-844, Helsinki, Finland.

Yue, Q., Guo, F., Kärnä, T., 2009. Dynamic ice forces of slender vertical structures due to ice crushing. Cold Reg. Sci. Technol., 56:77-83.

Yue, Q.J., Li, L., 2003. Ice problems in Bohai Sea oil exploitation. Proceedings of the 17th International Conference on Port and Ocean Engineering under Arctic Conditions, 13p, Trondheim, Norway.

Yue, Q., Zhang, X., Bi, X., Shi, Z., 2001. Measurements and analysis of ice induced steady state vibration. Proceedings of the 16th International Conference on Port and Ocean Engineering under Arctic Conditions, 413-421, Ottawa, Canada.